AN INVESTIGATION OF VIBRATION PHENOMENA IN TORSIONAL SYSTEMS HAVING NON-LINEAR SPRING CHARACTERISTICS

CARL ARTHUR PETERSON

An Investigation of Vibration Phenomena in Torsional Systems Having Non-Linear Spring Characteristics

By

Carl Arthur Peterson
B.S. (United States Naval Academy) 1929

THESIS

Submitted in partial satisfaction of the requirements for the degree of

MASTER OF SCIENCE

in

Mechanical Engineering

in the

GRADUATE DIVISION

of the

UNIVERSITY OF CALIFORNIA
(May, 1939)

Approved: C. H. Garland

C. T. Wilson

R. L. Folsom

Committee in Charge

AN INVESTIGATION OF VIBRATION PHENOMENA IN TORSIONAL SYSTEMS HAVING NON-LINEAR SPRING CHARACTERISTICS

Typed by Viola M. Priest

ACKNOWLEDGMENT

The writer wishes to express his sincere appreciation to Professor C. F. Garland for his invaluable advice, suggestions, criticism, and guidance throughout the course of this investigation.

Acknowledgment is also made of the many helpful suggestions and the close cooperation of Mr. W. F. Pemberton in the design and construction of equipment.

S U M M A R Y

In order to determine the effect of a non-linear spring characteristic on the vibrations of a torsional system, investigations were made to determine the response curves of a given system when the drive was made through a non-linear coupling and when made through a comparable shaft. The results showed the maximum amplitude for the former case to be about one-fourth of that for the latter. However, when the difference in damping was acounted for, the non-linear coupling showed a reduction in amplitude of vibration to about one-half that of the comparable linear system. An analytical solution including damping is given, and suggestions are made for further study.

TABLE OF CONTENTS

INTRODUCTION

While couplings having non-linear torque-deflection characteristics have been used for some time in installations where it is desired to reduce torsional vibrations, and while the accomplishment of this mission is generally conceded, there is no data available for evaluating their effectiveness in this regard. It is desirable, when considering an installation of this type, to know not only if an improvement will be realized, but also how much improvement. It was, therefore, with this point in mind that the subject investigation was undertaken.

APPARATUS

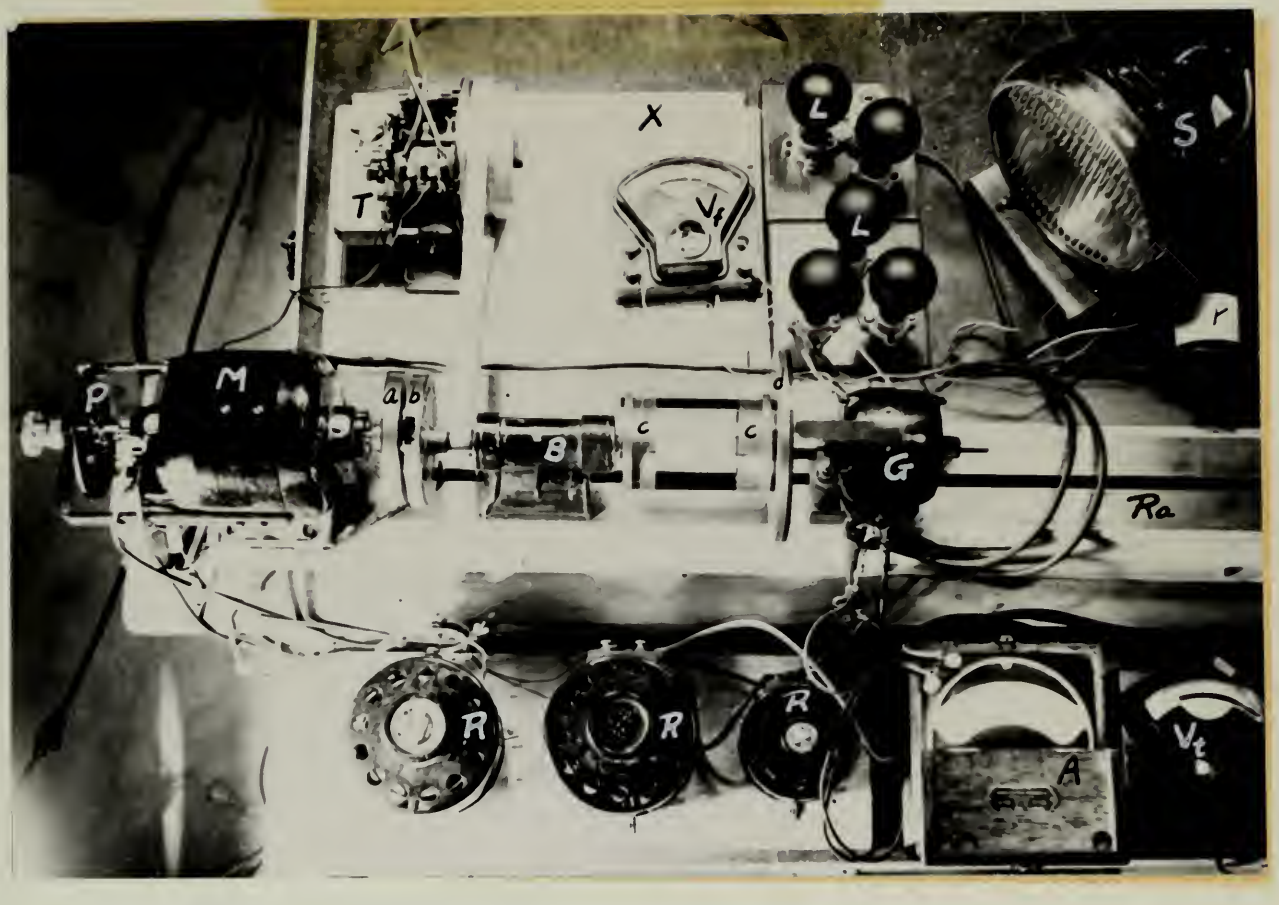

Fig. 1

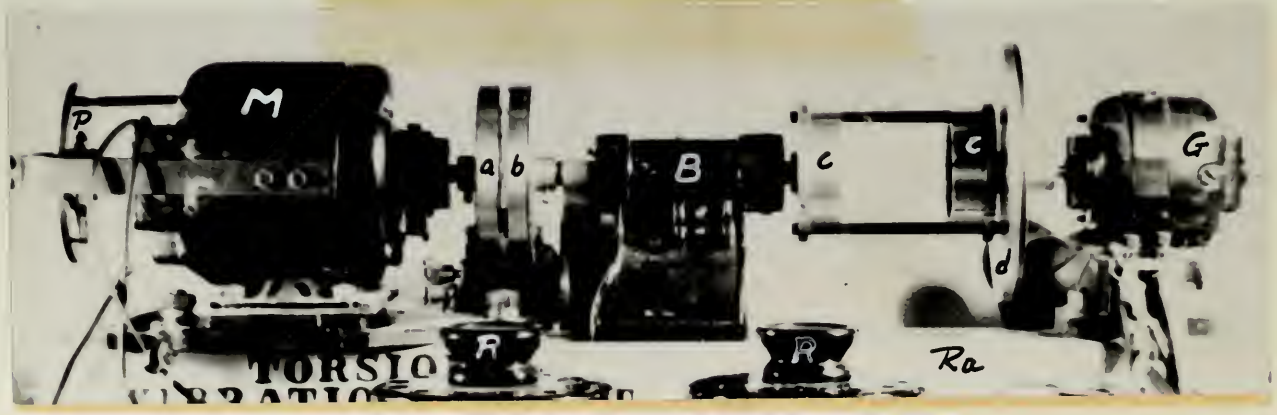

Fig. 2

A — ammeter (load amps.)

B — pedestal bearing

a - b — Whitworth drive

b — driving disc (referred to coupling), graduated 0-360 degrees

c - c — non-linear coupling

d — driven disc (referred to coupling), graduated 0-360 degrees

G — generator (d.c., 115 v., 1/20 H.P. at 1725 R.P.M.)

L — lampbank load

M — motor (d.c., 115 v., 2.43 amps., 1/4 H.P. at 1725 R.P.M.)

P — breaker points, attached to graduated dial

R — rheostats for speed control

r — rheostat for control of generator field

Ra — mounting rail

S — stroboscope

T — torsiograph

V_f — voltmeter (generator field voltage)

V_t — voltmeter (generator terminal voltage)

X — "strobotac" (not shown)

Power: 6 v. d.c.—for stroboscope and torsiograph

115 v. d.c.—for motor drive and generator field

115 v. 60 cycle a.c.—for strobotac

Fig. 3

Fig. 4

The Whitworth drive is an inversion of the slider crank mechanism designed to impress an oscillatory torque on disc "b". The offset between the shaft to "a" and the shaft from "b" was kept constant at 1/8" throughout.

The coupling used is shown in detail in Figures 3 and 4. It may be seen that the segments holding the spring strips are cut with first a plane portion and then a cylindrical portion. The radius of curvature of this latter part is 6 inches. The non-linearity is produced by the wrapping of the spring strips upon the cylindrical segments thus:

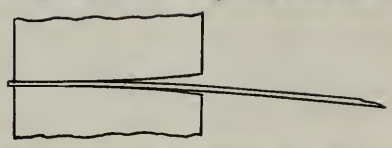

This shortens the unsupported length of the strip and so stiffens the coupling. The spring strips have a free sliding fit in the straight portion of the segments in order to allow for the axial motion necessary when the coupling is deflected. Clock-spring steel .025 inches thick and 3/8 inches wide was used for the spring strips. The "coupling lengths" referred to in the discussion to follow are the unsupported lengths of the spring strips when not deflected. This length was varied for the different runs by sliding the assembly "G", "d", and one coupling flange "c" toward the motor end of the set-up. The ends of the strips

were then cut off to allow only the slight projection beyond the coupling flanges shown in Figure 2. Parts "M", "B", and "G" were bolted rigidly to the mounting rail "Ra". For the runs made with ordinary linear shafts only the spring strips were removed from the set-up as shown in Figure 1. The coupling flanges "c" were allowed to remain in place and the shaft connected between them by means of chucks. Two intermediate bearings were used to support the shafts tested.

The shaft of motor "M" projects through the outboard bearing to within a short distance of disc "P". A cam on this shaft operates a set of breaker points mounted on "P", breaking the circuit through these points once each revolution. The primary of the stroboscope "S" is in series with this circuit, causing the stroboscope to flash each time the circuit is broken. By rotation of disc "P" to the desired position this flash may be made to occur at any position of the shaft during a revolution. A knurled locking nut is used to lock disc "P" in the position desired. The effect of this mechanism is to allow simultaneous readings to be taken of the position of discs "b" and "d" at various points throughout a revolution of "b", these points being determined by the setting of dial "P" which is graduated. Thus a scan may be made of these instantaneous positions throughout a revolution. A circuit from the breaker

points also operates the dead center timing pen of the torsiograph.

The torsiograph is driven by a belt from the shafting between "b" and "B". In order to reduce slippage this section of shafting was wound with friction tape. In this condition the shaft diameter was 11/16 inches. When running the linear shafts it was found that the amplitudes of vibration were too large to be recorded by the torsiograph as installed, even at its lowest amplification. This was remedied by driving the torsiograph from the test shaft itself, which provided the necessary smaller driving diameter. This shaft, taped, measured 7/32 inches.

The generator field was separately excited, the excitation being maintained at 100 volts. The lampbank load was not changed during the investigation; hence the load increased with the speed of operation. The lamps of the lampbank were painted black in order that they would emit no light.

The strobotac was mounted in the position indicated by "X" in Figure 1, so as to throw its light on the spring strips. When running the shafts, the strobotac was brought to the near side (in Figure 1) of the mounting rail and its light directed on that face of disc "d" which faces the coupling flanges. The strobotac was used for speed measurement only, and should not be confused with the stroboscope which was used in obtaining dial readings as described above.

For all runs involving the use of the stroboscope or the strobotac, the laboratory was made as dark as possible in order to facilitate the taking of readings.

PROCEDURE

PROCEDURE

With the apparatus set up as shown in Figure 1, a preliminary run was made to determine the speeds at which it would be desirable to take readings. This was done by increasing the motor speed by small increments, each time "stopping" the rotational motion of the coupling with the strobotac. In this state the amplitude of the vibratory motion in the coupling could be observed by eye. Speeds were thus chosen which gave desired increments of amplitude change. The critical speeds were also determined during this run.

The strobotac was then set at the lowest speed at which an amplitude determination was desired. The motor speed was adjusted, by means of the motor rheostats, until rotational motion of the coupling was "stopped" by the strobotac light. Since the speed of the motor had a tendency to vary, it was watched constantly and readings were taken only when the speed was steady and at the desired value. The rotation of the motor shaft caused the stroboscope to flash once each revolution, as previously explained. By the light of these flashes the dials on the driving and driven discs (designated as "b" and "d" in Figure 1) were read

and recorded. The corresponding setting of dial "P" was also recorded. Dial "P" was then rotated in increments of 15 degrees, thus causing the stroboscope to flash at successive positions during the cycle. Readings of dials "b" and "d" were taken for each position. When a complete cycle of readings had been obtained the voltmeter and ammeter readings were recorded and a record of the motion of disc "b" taken on the torsiograph. The speed was then increased to the next desired value and the procedure repeated. Readings were thus taken at speeds ranging as close to the critical speed as possible. Readings at the critical speed were not possible due to the difficulty of maintaining constant speed. After passing the critical, the speed was increased to the maximum value at which readings were desired, and then reduced in steps, taking readings at each step as before. This was continued until the point of instability at decreasing speed was reached.

The motor was then stopped and a reading taken of the relative position of dials "b" and "d" with no twist in the coupling. This served as a reference reading in determining the actual position of one disc, relative to the other, from the readings previously taken.

Following this a bar was attached to the shaft between "B" and "c" and the end of the generator shaft was rigidly clamped to prevent turning, by means of a pedestal

secured to the mounting rail. Using a spring scale known increments of torque were applied to the shaft and the resulting angular deflection read from dial "b". This was done for increasing and decreasing values of torque to obtain data for the hysteresis loop of the unit. This completed the readings taken for a given coupling length.

The entire procedure was repeated for each of the coupling lengths.

The procedure for each of the shafts (i.e., "linear couplings") tested was identical, with the exception that the hysteresis loop was taken before the run in order to determine that the shaft stiffness was of the desired magnitude. This stiffness was also checked after the run to assure that no change had occurred due to the stress of the large deflections encountered.

Due to the small output of the generator and the difficulty of determining its efficiency at this light load, a series of runs was made with the motor and generator coupled through a short, stiff shaft. The input to the motor was determined with no load and no field on the generator, and again determined with the load and field adjusted to that used in making the coupling runs. The difference was assumed to be the load input to the generator. This difference was determined for various speeds

and the results plotted (see Figure 18). While the accuracy of this procedure is not good, it is considered satisfactory inasmuch as it contributes only a small fraction of exciting torque applied to the driving disc.

THEORY

T H E O R Y

1. Notation

a = component of steady state amplitude, see definition of s and y.

b = viscous damping factor, pound inch seconds per radian.

c = component of steady state amplitude, see definition of s and y.

e = the eccentricity between discs "a" and "b".

I = moment of inertia of mass or combination of masses indicated by subscript, see Figure 5.

I_E = mass moment of inertia of equivalent system $= \frac{I_1 I_2}{I_1 + I_2}$

k = torsional stiffness of shaft, pound inches per radian.

k_1 = initial slope of non-linear torque-deflection curve.

k_2 = coefficient of the cubed term in the expression for the non-linear torque-deflection curve.

$K = 3/4 \ \frac{k_2}{k_1}$

$n = \frac{b}{2I_E}$

N = rotational speed in revolutions per minute = $\frac{30}{\pi} \omega_f$

N_n = natural frequency expressed in revolutions per minute = $\frac{30}{\pi} \omega_n$

$p = \frac{r}{e}$

r = the crank radius of the Whitworth linkage.

R = frequency ratio = $\frac{\omega_f}{\omega_n} = \frac{N}{N_n}$

$S = y^2 = a^2 + c^2$

$T_a = T_L + T_D$

T_b = the coefficient of the sinusoidal component of driving torque applied to disc "b".

T_b' = total driving torque applied to disc "b".

T_D = damping torque.

T_E = equivalent torque = $\frac{I_1 I_2}{I_1 + I_2}$

T_L = load torque.

T_I = inertia torque.

$T_1 = T_I + T_b$

y = angle of twist in radians.

$y_{st} = \frac{T_E}{k_1}$

β = "amplification factor" = $\frac{1}{\sqrt{(1-R^2)^2 + \gamma^2 R^2}}$

γ = dimensionsless damping coefficient = $\frac{b}{I \omega_n} = \frac{2n}{\omega_n}$

ϕ = angle of twist in degrees.

ω_f = circular frequency of forced vibration.

ω_n = natural frequency = $\sqrt{\frac{k_1}{I_E}}$

2. Derivation of amplitude equation

In order to reduce the complexity of the analysis the system must first be simplified. The steps of this simplification may be indicated as follows:

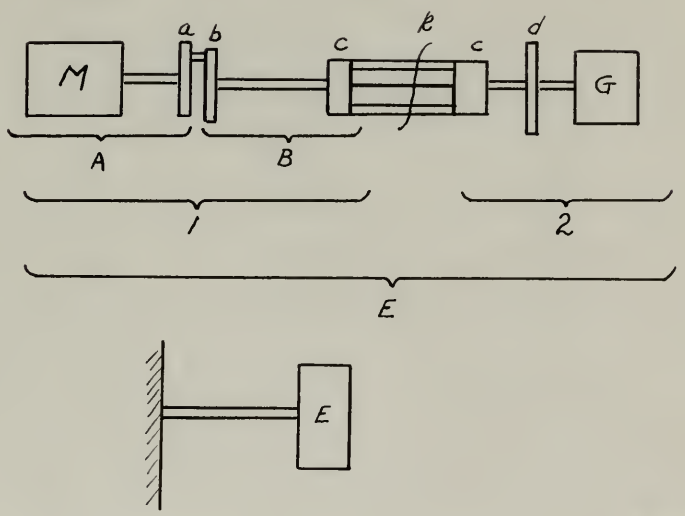

Figure 5

The letters indicating the original masses of the system above are the same as those employed to designate these parts in Figures 1 and 2.

Since the masses "M" and "a" are rigidly connected,

$$I_A = I_M + I_a$$

likewise,

$$I_B = I_b + I_c$$

and $I_2 = I_c + I_d + I_G$

Equating the kinetic energies of system 1 and its component parts:

$$1/2\ I_A\ \omega^2_{A_{av.}} + 1/2\ I_B \omega^2_{B_{av.}} = 1/2\ I_1\ \omega^2_{av.}$$

But $\omega_{A_{av.}} = \omega_{B_{av.}} = \omega_{av.}$

$\therefore\ I_1 = I_A + I_B$

We now have a two mass system with moments of inertia I_1 and I_2, connected by a spring of stiffness k.

Let a periodic torque of magnitude T_1 be applied to mass 1. Then it may be shown (Reference 1, page 33) that the equation of motion of the two mass system is:

$$\frac{I_1 I_2}{I_1 + I_2}\ \ddot{y} + b\dot{y} + ky = \frac{I_2 T_1}{I_1 + I_2}\ f(\omega_f t)$$

Where y = the relative motion between discs "b" and "d" (viz., the angle of twist).

This equation is identical with the equation of absolute motion of the system E if

$$I_E = \frac{I_1 I_2}{I_1 + I_2}$$

and $T_E = \frac{I_2 T_1}{I_1 + I_2}$

Therefore we may write as the equation of motion of the equivalent system:

$$I_E\ddot{y} + b\dot{y} + ky = T_E\, f(\omega_f t) \qquad (1)$$

$T_E\, f(\omega_f t)$ may be written as a Fourier series, the motion due to each component evaluated, and the net resultant motion obtained by superposition. From this point on we therefore will consider only the fundamental component $T_E \sin \omega_f t$, which satisfactorily describes this torque for the case under consideration.

In the case of a linear system (k = constant), we have a linear differential equation, which may be solved for y, giving the well known expression for maximum amplitude:

$$y_{max} = \frac{T_E/k}{\sqrt{(1-R^2)^2 + \gamma^2 R^2}} = \beta\,(T_E/k)$$

However, for the non-linear system [k = f(y)] no such simple general solution exists. The following derivation is based on an article by Appleton (Reference 2).

First, it is assumed that the torque deflection curve of the torsional spring can be expressed by an equation of the form:

$$T = k_1 y + k_2 y^3$$

The choice of this form of expression for the spring characteristic is arbitrary, and is chosen primarily for conveni-

ience. However, results of this investigation show it to give satisfactory agreement with the actual curves obtained.

Substituting this expression for our spring torque into equation (1) we have:

$$I_E\ddot{y} + b\dot{y} + k_1 y + k_2 y^3 = T_E \sin \omega_f t, \qquad (2)$$

or $$I_E\ddot{y} + b\dot{y} + k_1 y \left(1 + \frac{k_2}{k_1} y^2\right) = T_E \sin \omega_f t .$$

Dividing by I_E, we obtain:

$$\ddot{y} + \frac{b}{I_E}\dot{y} + \frac{k_1}{I_E} y \left(1 + \frac{k_2}{k_1} y^2\right) = \frac{T_E}{I_E} \sin \omega_f t$$

or $$\ddot{y} + 2n\dot{y} + \omega_n^2 y \left(1 + \frac{k_2}{k_1} y^2\right) = \omega_n^2 y_{st} \sin \omega_f t, \qquad (3)$$

where $$2n = \frac{b}{I_E} ,$$

$$\omega_n^2 = \frac{k_1}{I_E} ,$$

and $$y_{st} = \frac{T_E}{k_1} .$$

Neglecting the transient term, let the trial solution be:

$$y = a \sin \omega_f t + c \cos \omega_f t \qquad (4)$$

then $$\dot{y} = a\,\omega_f \cos \omega_f t - c\,\omega_f \sin \omega_f t \qquad (5)$$

and $\ddot{y} = - a \omega_f^2 \sin \omega_f t - c \omega_f^2 \cos \omega_f t$ (6)

In considering the non-linear term involving y^3, we shall, as a first approximation, neglect the influence of the harmonics and retain only those terms involving ω_f.

Thus cubing equation (4), reducing terms to first power functions of $\omega_f t$, and discarding all functions of $2\omega_f t$, $3\omega_f t$, we obtain:

$$y^3 = 3/4\, a^3 \sin \omega_f t + 3/4\, a^2 c \cos \omega_f t + 3/4\, ac^2 \sin \omega_f t + 3/4\, c^3 \cos \omega_f t \quad (7)$$

Substituting $\dot{y}$, $\ddot{y}$ and y^3 from equations (5), (6), and (7) into equation (3) and equating the coefficients of the sine and cosine terms respectively, we have:

$$-a\omega_f^2 - 2nc\omega_f + \omega_n^2 a + 3/4\, \omega_n^2\, a \frac{k_2}{k_1} (a^2 + c^2) = \omega_n^2\, y_{st} \quad (8)$$

$$-c\omega_f^2 + 2na\omega_f + \omega_n^2 c + 3/4\, \omega_n^2\, c \frac{k_2}{k_1} (a^2 + c^2) = 0$$

Rewriting:

$$a (\omega_n^2 - \omega_f^2) - 2n\omega_f c + 3/4\, \omega_n^2\, \frac{k_2}{k_1}\, a (a^2 + c^2) = \omega_n^2\, y_{st} \quad (9)$$

$$c (\omega_n^2 - \omega_f^2) + 2n\omega_f a + 3/4\, \omega_n^2\, \frac{k_2}{k_1}\, c (a^2 + c^2) = 0$$

Let $R = \frac{\omega_f}{\omega_n}$,

$\gamma = \frac{2n}{\omega_n}$,

$K = 3/4 \frac{k_2}{k_1}$.

Substituting these relationships into (9), we obtain:

$$a(1-R^2) - \gamma Rc + aK(a^2 + c^2) = y_{st}$$

$$c(1-R^2) + \gamma Ra + cK(a^2 + c^2) = 0$$

Rearranging:

$$\begin{aligned} [\ 1 - R^2 + K\ (a^2 + c^2)\ ]\ a - \gamma Rc &= y_{st} \\ [\ 1 - R^2 + K\ (a^2 + c^2)\ ]\ c + \gamma Ra &= 0 \end{aligned} \qquad (10)$$

Let $S = a^2 + c^2$ = the square of the amplitude for steady state conditions.

Substituting and operating on (10):

$$(1 - R^2 + KS)^2 a^2 - 2(1 - R^2 + KS)a\ \gamma Rc + \gamma^2 R^2 c^2 = y_{st}^2$$

$$(1 - R^2 + KS)^2 c^2 + 2(1 - R^2 + KS)c\ \gamma Ra + \gamma^2 R^2 a^2 = 0$$

Adding:

$$(1 - R^2 + KS)^2 S + \gamma^2 R^2 S = y_{st}^2 \qquad (11)$$

This is a cubic equation in S, the real roots of which will

give values of the possible steady state amplitudes. The criteria for stability of these amplitudes will not be discussed here since the regions of stability and instability of the non-linear response curve are well known and are covered in most vibration texts.

Since solution of a cubic equation is unhandy, S may be made the independent variable and the equation expressed as a quadratic in R^2.

Rewriting equation (11):

$$\left[(1 + KS) - R^2 \right]^2 + \gamma^2 R^2 = y^2_{st/S}$$

$$(1 + KS)^2 - 2(1 + KS)R^2 + R^4 + \gamma^2 R^2 - y^2_{st/S} = 0$$

$$R^4 - 2(1 + KS - \gamma^2/2)R^2 - y^2_{st/S} + (1 + KS)^2 = 0$$

whence

$$R^2 = KS+(1-\gamma^2/2) \pm \sqrt{K^2S^2+ 2(1-\gamma^2/2)\, KS+(1-\gamma^2/2)^2 +y^2_{st/S} - 1- 2KS - K^2S^2}$$

$$R^2 = KS + (1 - \gamma^2/2) \pm \sqrt{y^2_{st/S} - \gamma^2 KS + (1 - \gamma^2/2)^2 - 1} \qquad (12)$$

Equation (12) is the expression used in the computation of the non-linear coupling response curves. It lends itself readily to a computing form.

3. Other theoretical considerations

(a) Evaluation of T_E

From the preceding derivation:

$$T_E = \frac{T_1 I_2}{I_1 + I_2}$$

The net torque exerted by the motor must be equal to the resisting torque of the generator plus the damping torque, T_L and T_D respectively. This net torque is a constant at disc "a", but in being transmitted through the linkage of the Whitworth drive acquires an oscillatory component. From the mechanics of the system it may be determined that

$$T_b' = T_a \frac{p^2 - 2p \cos(\omega t) + 1}{p^2 - p \cos(\omega t)}$$

where $p = \frac{r}{e}$

r = the distance of the driving pin of the linkage from the center of disc "a", equal to 1.5 inches for this installation.

e = the eccentricity between discs "a" and "b", equal to 0.125 inches for all runs made.

$T_a = T_L + T_D$

T_b' = total driving torque applied to disc "b".

Evaluating the constants and expressing as a series we have:

$$T_b' = T_a(1.00-.083 \cos \omega t - .003 \cos 2\omega t - .0001 \cos 3\omega t + ...)$$

Discarding the harmonics above the first as negligible, there remains, superimposed on the constant torque, a simple sinusoidal torque of maximum amplitude:

$$T_b = .083 (T_L + T_D)$$

Since vibrations of the masses "B" may be transmitted through the Whitworth drive to masses "A", the latter will be caused to oscillate also. These oscillations result in an inertia torque being impressed on disc "b". Designating this torque as T_I' we may write:

$$T_I' = I_A \alpha_A$$

Again by the mechanics of the Whitworth drive, substituting the constants used above, we have:

$$\alpha_A = \omega_b^2 (.083 \sin \omega t + .007 \sin 2\omega t + .0003 \sin 3 \omega t + ...)$$

Neglecting the harmonics higher than the first and substituting above we obtain:

$$T_I' = .083 \omega_b^2 I_A \sin \omega t$$

Or, designating the maximum amplitude of the sinusoidal torque as T_I, and noting that ω_b is the same as the speed of rotation of the coupling (viz., ω_f), we have:

$$T_I = .083\ \omega_f^2\ I_A$$

The oscillatory component of the torque applied to system "1" will be the sum of the oscillatory component of the driving torque plus the inertia torque. This will be a sinusoidal torque of maximum amplitude:

$$T_1 = T_I + T_b$$

Substituting in the expression for T_E, we have:

$$T_E = \left[.083\ \omega_f^2\ I_A + .083\ (T_L + T_D)\right] \frac{I_2}{I_1 + I_2}$$

$$= \left[.083\ \omega_f^2\ (I_M + I_A) + .083\ (T_L + T_D)\right] \frac{I_2}{I_1 + I_2}$$

T_L is evaluated from a speed vs. load-torque curve.

T_D is evaluated from the hysteresis loop for the particular set-up being considered.

(b) Evaluation of the damping factor, γ .

The damping factors used in the computations for both the shafts and the non-linear couplings were so deter-

mined as to make the maximum amplitude of the theoretical curves at resonance the same as that observed. Although this is apparently a subterfuge, its use will be defended in the discussion to follow.

For the linear system at resonance, $\gamma = \frac{1}{\beta}$ and may be determined by computing backwards from a given maximum amplitude.

For the non-linear system γ may be determined as follows:

Differentiating equation (11) with respect to R, we obtain:

$$\left[(1 - R^2) + KS\right]^2 \frac{dS}{dR} + 2S\left[(1 - R^2) + KS\right](-2R + K\frac{dS}{dR}) + \gamma^2 R^2 \frac{dS}{dR} + 2\gamma^2 RS = 0$$

$$\frac{dS}{dR}\left[(1 - R^2)^2 + 2KS(1 - R^2) + K^2S^2 + 2KS(1 - R^2) + 2K^2S^2 + \gamma^2R^2\right] = 4RS\left[(1 - R^2) + KS - \frac{\gamma^2}{2}\right]$$

or:

$$\frac{dS}{dR} = \frac{2RS(2 - 2R^2 + 2KS - \gamma^2)}{(1 - R^2)^2 + \gamma^2R^2 + 4KS(1 - R^2) + 3K^2S^2}$$

The maximum point on the resonance curve occurs when the slope is zero. Since R and S are not zero, it is necessary that:

$$2 - 2R^2 + 2KS - \gamma^2 = 0$$

or

$$1 - R^2 + KS - \gamma^2/2 = 0$$

Substituting for R^2 from equation (12):

$$1 - KS - 1 + \gamma^2/2 \mp \sqrt{y^2_{st/S} - \gamma^2 KS + (1 - \gamma^2/2)^2 - 1} + KS - \gamma^2/2 = 0$$

whence

$$y^2_{st/S} - \gamma^2 KS + (1 - \gamma^2/2)^2 - 1 = 0$$

$$y^2_{st/S} - \gamma^2 KS + 1 - \gamma^2 + \gamma^4/4 - 1 = 0$$

$$\gamma^4/4 - (KS + 1)\gamma^2 + y^2_{st/S} = 0$$

$$\gamma^2 = 2\left(KS + 1 \pm \sqrt{(KS + 1)^2 - y^2_{st/S}}\right) \qquad (13)$$

D I S C U S S I O N

DISCUSSION

Since the comparison of the non-linear with the linear system was made on the basis of an "equivalent shaft" it is necessary first to define this term. This definition follows: "A shaft is considered equivalent to a given coupling when the slope of its torque-deflection curve is the same as the initial slope of the torque-deflection curve of the given coupling." On this basis the initial flexibility of a coupling and its equivalent shaft is the same (i.e., k of the shaft equals k_1 of the coupling). Thus the two systems are brought together at an initial point. Departure of the behavior of one system from that of the other as operation occurs removed from this point (viz., amplitude of vibrations become greater than zero) must be due to whatever difference exists in the spring characteristics and the damping of the two systems, since the moments of inertia remain essentially the same.

As the purpose of this investigation was to determine the effect of the non-linear spring characteristic, it would have been desirable to make the damping of the two systems identical. However, no attempt was made to do this, and it will therefore be necessary to estimate the effect

of the difference in damping in order to draw a conclusion as to the effect due solely to the non-linearity of the spring. It is doubtful that a coupling could have been designed such that the damping in the coupling system and in the equivalent shaft system would have been identical. In neither case was the damping purely viscous; rather it was of some complex type, evaluation of which would have been quite difficult. Following accepted practice, the damping was expressed as an equivalent viscous damping, in amount equal to that necessary to give the observed maximum amplitude at resonance. The method of making this evaluation for each system has been explained under "theoretical considerations." It is believed that the major cause of discrepancy between theoretical and observed values of amplitude is due to this approximate means of evaluating the damping, and it is therefore suggested that if future investigations are undertaken, they be directed primarily toward a more accurate solution of this problem.

Accepting the damping determined as described above, it was still necessary to arrive at some basis of comparison which would present the true effect of the non-linear spring characteristic alone. Since the damping in the coupling was much greater than that in the shaft, it is obvious that a comparison neglecting the difference in damping would present the former in too favorable a light. Therefore a theoretical

maximum amplitude was computed using the values of damping and torque at resonance of the equivalent shaft. The maximum amplitude thus obtained was almost double that observed, but still about half the maximum amplitude of the equivalent shaft, as may be seen in Figures 6 to 9 inclusive.

Damping also complicated the evaluation of the torque-deflection curve of the non-linear system. Since the deflection was changed very slowly in obtaining the curve, the only damping present was that independent of the speed, viz., Coulomb damping. The result of its presence, however, was to give a hysteresis loop rather than a single curve. Inspection of the curve indicates that the friction was greater with decreasing torque than with increasing torque. Thus we have the spring characteristic confused with part of the damping. The true spring characteristic must lie somewhere within the loop. A characteristic evaluated to pass through the maximum point of the hysteresis loop was found to be unsatisfactory since, at the larger angles of twist, conditions are such as to make the damping effect overshadow the spring effect on the curve. Similarly, the mean line between the two boundaries of the loop was found to give poor results because it was unduly lowered by the increased damping effect of the descending branch of the curve. By trial it was found that a curve approximately parallel to the upper branch of the hysteresis loop, passing

through the origin, gave the most uniformly satisfactory results. Since the initial slope of the approximate curve represented by the cubic equation is fixed (it is equal to the initial slope of the upper branch of the hysteresis loop), it can be forced to coincide with the actual curve at only one point other than the origin. This coincidence was made approximately at the mid-point of the actual torque-deflection curve. Since the actual curve itself is at best only an estimate as shown above, a small departure from it by the approximate curve is not considered serious.

Referring to equation (12), it should be noted that T_E is a function of ω_f (or of N), which is in turn a function of R. The equation is thus not in proper form for evaluation as a quadratic. However, a value of N may be estimated, from which T_E may be computed. If the value of R thus determined gives an N which differs by more than 10 per cent from the N estimated, the computed N may be used for the next estimate and the value of R recomputed. If there is no other means of estimating N for the first approximation, the value of N_n (which is known for any particular system) may be used for all but the lowest amplitudes. If the first estimate of N is considerably lower than the actual value, the quantity under the radical becomes negative, giving a complex number for R^2. In general, knowing the value of N_n, and having a knowledge of the gen-

eral shape of non-linear response curves, a sufficiently satisfactory estimate can be made so that not more than two approximations are necessary. A 10 per cent variation in the estimated value of N will give approximately a 1 per cent variation in the computed value of N. From this it is apparent that the result is not being forced by the estimate. If equation (//) had been solved as a cubic in S it would not have been necessary to make the above approximations since in that case R would be the independent variable. It is considered, however, that the above method lends itself more readily to mass calculation (i.e., a computing form).

The observed amplitudes indicated on the response curves, Figures 6 to 9 inclusive, were obtained directly from the readings of dials "b" and "d" and represent the angle of twist from the mean position, viz., half the sum of the maximum angles of twist in each direction.

It is interesting to note that in the cases where the non-linearity is most pronounced, the overlap of the upper and lower branches of the response curves is sufficient to allow advantage to be taken of the effect, as follows: If it is desired to run at a speed approaching the critical, increase the speed first until the critical is passed, then reduce the speed to that desired. Thus the machine may be made to operate on the lower branch of the curve where the amplitude is much smaller.

CONCLUSIONS

CONCLUSIONS

The results of this investigation indicate that a non-linear spring characteristic in a torsional system is effective in reducing the maximum amplitude of vibrations. An exact determination of the magnitude of this reduction was complicated by the existence of complex damping in the systems compared. However, a reasonable approximation seems to be that for systems of the type investigated the non-linearity will cause a reduction of about 50 per cent in the maximum amplitude from that of the comparable linear system.

It was also demonstrated that in a non-linear system advantage may be taken of the overlap of the upper and lower branches of the response curves to further reduce the maximum amplitude which must be accepted when operating in the critical zone. For the cases considered this additional reduction amounted to about 20 per cent of the maximum amplitude indicated by the non-linear response curve. Referring to Figures 6 to 9 inclusive, it is seen that the response curve of the non-linear system shows appreciable amplitude over a wider range of frequencies than does that of the linear system. However, the great reduction effected in peak amplitude is considered to more than compensate for this disadvantage in most installations.

REFERENCES

RKFERENCES

1. "Mechanical Vibrations," by J. P. Den Hartog, McGraw-Hill Book Company, Inc., New York, 1934.

2. "On the Anomalous Behavior of a Vibration Galvanometer," by E. V. Appleton, Philosophical Magazine, Vol. 47, 1924.

APPENDIX I

APPENDIX I

Sample Calculations

In the following we shall consider first some general calculations used for all computations. Following this, sample calculations for the 4-1/3 inch coupling are presented, together with those for its equivalent shaft. Finally, computations are made for the theoretical maximum amplitude considering the shaft torque and damping to be applied to the coupling system.

General Calculations

$$I_1 = I_A + I_B$$

$$= I_M + I_a + I_b + I_c$$

$$= .01709 + .02650 + .02354 + .01085$$

$$= .078 \text{ slug in.}^2$$

$$I_2 = I_c + I_d + I_G$$

$$= .01085 + .06594 + .00125$$

$$= .078 \text{ slug in.}^2$$

$$I_E = \frac{I_1 I_2}{I_1 + I_2}$$

$$= \frac{.078 \times .078}{.078 + .078} = .039 \text{ slug in.}^2$$

$$T_E = \frac{I_2 T_1}{I_1 + I_2} = \frac{.078 \quad T_1}{.078 + .078} = \frac{T_1}{2}$$

Calculations for the 4-1/3 inch coupling

Evaluation of the approximate torque-deflection curve.

From Figure 11, the initial slope of the torque-deflection curve is:

$k_1 = .53\#$ in./o x 57.3 = 30.4# in./rad.

and $T = 17.6\#$ in. when $\phi = 20^o$.

$$y = \frac{20}{57.3} = .349 \text{ radians}$$

$$T = k_1(y + \frac{k_2}{k_1} y^3)$$

$$17.6 = 30.4 \ (.349 + \frac{k_2}{k_1} \times \overline{.349}^3 \ )$$

$$\frac{k_2}{k_1} = 5.43$$

$$K = 3/4 \frac{k_2}{k_1} = 3/4 \times 5.43 = 4.1$$

Determination of the natural frequency.

$$\omega_n = \sqrt{\frac{k_1}{I_E}} = \sqrt{\frac{30.4}{.039}} = 28 \text{ rad./sec.}$$

$$N_n = \frac{30}{\pi} \omega_n = 268 \text{ r.p.m.}$$

Evaluation of the damping.

The maximum amplitude observed for this coupling was 29.5° at N = 387.

$$\omega_f = \frac{\pi}{30} N = \frac{387\pi}{30} = 40.5 \text{ rad./sec.}$$

$$T_E = .083 \left[\omega_f^2 (I_M + I_a) + (T_L + T_D) \right] \frac{I_2}{I_1 + I_2}$$

$$= .083 \left[\overline{40.5}^2 (.01709 + .02650) + (2.50 + 1.20) \right] x\frac{1}{2}$$

$$= 3.15\# \text{ in.}$$

$$y_{st} = \frac{T_E}{k_1} = \frac{3.15}{30.4} = .1036$$

$$y_{st}^2 = .0107$$

$$y_{max} = \frac{29.5}{57.3} = .514$$

$$S_{max} = y_{max}^2 = \overline{.514}^2 = .264$$

$$\frac{y_{st}^2}{S_{max}} = \frac{.0107}{.264} = .0404$$

$$\gamma^2 = 2\left(KS + 1 \pm \sqrt{(KS + 1)^2 - y^2_{st/S}}\right) \qquad (13)$$

Substituting:

$$\gamma^2 = 2\left(4.1 \times .264 + 1 \pm \sqrt{(4.1 \times .264 + 1)^2 - .0404}\right)$$

$$\gamma^2 = .0196$$

$$\gamma = .1400$$

Evaluating the response curve:

$$R^2 = KS + (1 - \gamma^2/2) \pm \sqrt{y^2_{st/S} - \gamma^2 KS + (1 - \gamma^2/2)^2 - 1} \qquad (12)$$

Substituting:

$$R^2 = 4.1S + .990 \pm \sqrt{\frac{T_E^2}{923S} - .08S - .020}$$

We may now substitute values for S and solve for R^2.

For convenience, take the amplitude y = .1 radian ($\phi = 5^{\circ}.73$).

Then $S = y^2 = .01$

To evaluate T_E it is necessary to estimate a value of N.

A substantiation of this procedure is given in the discussion.

For y = .1 , for the upper branch of the response curve

$$N_{est} = 220 \text{ RPM}$$

For the lower branch of the response curve

$$N_{est} = 370 \text{ RPM}$$

Proceeding for the upper branch of the response curve:

$$T_E = .083 \left[\omega_f^2 (I_M + I_a) + (T_L + T_D)\right] \frac{I_2}{I_1 + I_2}$$

$$= .083 \left[\left(\frac{220\pi}{30}\right)^2 (.0436) + 2.76\right] \times \frac{1}{2}$$

$$= 1.09$$

T_L and T_D were obtained from Figs. 18 and 11 respectively.

Substituting in the equation for R^2 and using the negative sign before the radical since the lower of the two values for R^2 is desired:

$$R^2 = 4.1 \times .01 + .990 - \sqrt{\frac{1.09^2}{923 \times .01} - .08 \times .01 - .020}$$

$$= 1.031 - .3289$$

$$= .7021$$

$$R = \sqrt{.7021} = .837$$

$$N = RN_n = .837 \times 268 = 225 \text{ RPM}$$

Proceeding similarly for the lower branch of the response curve, and using the positive sign before the radical, we obtain:

$$N = 374$$

Thus two points on the response curve have been obtained,

viz.:

$$\phi = 5.^{\circ}73, \quad N = 225$$

$$\phi = 5.^{\circ}73, \quad N = 374$$

Following the same procedure sufficient points may be obtained to determine the theoretical response curve for the 4-1/3 inch coupling given in Fig. 7.

Computations for the equivalent shaft.

Using calculations given above for the coupling:

$$k = k_1 = 30.4 \ {}^{\#in}/_{rad}$$

$$\omega_n = 27.8 \text{ rad/sec}$$

$$N_n = 268$$

At resonance:

$$T_E = .083 \left[\left(\frac{268\,\pi}{30} \right)^2 (.0436) + 3.08 \right] \times 1/2 = 1.54$$

$$\phi_{obs.} = 100^{\circ}$$

$$y = \frac{100}{57.3} = 1.747 \text{ rad.}$$

$$R = 1.0$$

$$\beta = \frac{1}{\gamma}$$

$$y_{max} = \beta \left({}^{T_E}/_{k} \right)$$

$$1.747 = \frac{1.54}{30.4\,\gamma}$$

$$\gamma = .0292$$

Values for the response curve may now be computed:

Determine the amplitude at N = 250:

$$T_E = 1.35 \quad , \quad R = \frac{250}{268} = .933 \quad , \quad R^2 = .870$$

$$y_{max} = \frac{T_E/k}{\sqrt{(1 - R^2)^2 + \gamma^2 R^2}}$$

$$= \frac{1.35/30.4}{\sqrt{(1 - .87)^2 + .0292^2 \times .870}}$$

$$= .334 \text{ rads.}$$

$$\phi = .334 \times 57.3 = 19^{\circ}.1$$

This gives one point on the linear response curve of Fig. 7. Other points may be determined similarly.

Computations for the theoretical maximum amplitude of the non-linear system when the torque and damping at resonance of its equivalent linear system is applied to it.

From previous computations -

$$T_E = 1.54$$

$$\gamma = .0292$$

Under "theoretical considerations" it was shown that

at maximum amplitude of the non-linear response curve -

$$\gamma^4/_4 - (KS + 1)\ \gamma^2 + y_{st}^2/_S = 0$$

Substituting and solving for S -

$$\frac{\overline{.0292}^4}{4} - (4.1S + 1) \times \overline{.0292}^2 + \frac{1.54}{923S} = 0$$

$$S = .728$$

$$y = \sqrt{S} = .853 \text{ radians}$$

$$\phi = .853 \times 57.3 = 48^{\circ}.9 \qquad \text{See Fig. 7}$$

APPENDIX II

Data

Moments of inertia:

I_M = .01709 slug in^2.

I_G = .00125 " "

I_a = .02650 " "

I_b = .02354 " "

I_c = .01085 " "

I_d = .06594 " "

"Equivalent" shafts:

All "equivalent" shafts were of mild steel, 3/16 inches diameter. The lengths were as follows:

38	inch	shaft	equivalent	to	4	inch	coupling
45-1/2	"	"	"	"	4-1/3	"	"
50-5/8	"	"	"	"	4-2/3	"	"
60-7/8	"	"	"	"	5	"	"

TABULATION OF CONDENSED DATA AND CORRESPONDING COMPUTED VALUES

4 inch Coupling			4-1/3 inch Coupling		
Frequency	Observed Amplitude	Computed Amplitude	Frequency	Observed Amplitude	Computed Amplitude
N-RPM	∅-degrees	∅-degrees	N-RPM	∅-degrees	∅-degrees
250A	4.5	5.8	200A	3.5	3.5
300A	11.5	11.5	250A	8.0	9.5
340A	17.5	16.3	290A	14.0	14.5
350A	19.5	17.5	300A	19.5	17.7
400A	22.0	23.5	320A	23.5	20.7
425A	25.0	26.0	340A	25.5	23.7
430A	26.0	26.3	360A	26.5	26.5
380D	10.0	9.0	370A	28.0	28.0
400D	7.0	7.0	380A	29.5	29.1
450D	4.5	5.0	383A	29.5	29.4
			340D	12.5	9.5
			350D	8.5	8.0
			400D	5.0	5.0

38 inch Shaft			46-1/2 inch Shaft		
Frequency	Observed Amplitude	Computed Amplitude	Frequency	Observed Amplitude	Computed Amplitude
N-RPM	∅-degrees	∅-degrees	N-RPM	∅-degrees	∅-degrees
260	8.0	7.7	200	3.5	3.5
265	13.0	12.3	240	12.0	12.0
275	27.5	18.5	250	20.5	19.7
283	56.5	37.5	260	47.5	55.0
305	16.5	32.5	285	18.0	19.3
325	11.0	15.5	300	12.5	13.3
370	7.5	7.5	400	5.0	5.0
400	5.0	5.7			
450	4.0	4.0			

Note: "A" indicates operation on upper branch of non-linear response curve.

"D" indicates operation on lower branch of non-linear response curve.

TABULATION OF CONDENSED DATA AND CORRESPONDING COMPUTED VALUES

4-2/3 inch Coupling			5 inch Coupling		
Frequency	Observed Amplitude	Computed Amplitude	Frequency	Observed Amplitude	Computed Amplitude
[illegible]	β-degrees	β-degrees	[illegible]	β-degrees	β-degrees
200A	3.5	4.6	200A	3.5	6.4
230A	7.0	9.2	225A	9.0	10.5
260A	14.5	14.5	250A	17.0	14.7
290A	24.0	19.8	275A	19.5	19.0
310A	26.0	23.2	300A	22.5	23.5
325A	28.5	25.5	310A	23.5	24.5
335A	28.0	27.0	320A	25.5	25.5
315D	9.0	9.0	300D	9.0	8.2
350D	5.5	5.5	340D	6.0	5.6
400D	4.0	4.0	385D	5.0	4.8

50-5/8 inch Shaft			60-7/8 inch Shaft		
Frequency	Observed Amplitude	Computed Amplitude	Frequency	Observed Amplitude	Computed Amplitude
[illegible]	β-degrees	β-degrees	[illegible]	β-degrees	β-degrees
200	5.0	4.2	140	2.5	2.2
230	12.0	13.3	210	9.5	14.2
240	24.0	23.5	220	34.0	23.0
245	43.5	41.0	230	62.0	76.0
249	72.0	76.0	250	20.5	23.0
265	19.5	31.0	265	11.0	14.0
275	15.5	18.7	350	5.0	5.0
300	9.0	10.0			
350	5.5	5.5			

Note: "A" indicates operation on upper branch of non-linear response curve.

"D" indicates operation on lower branch of non-linear response curve.

APPENDIX III

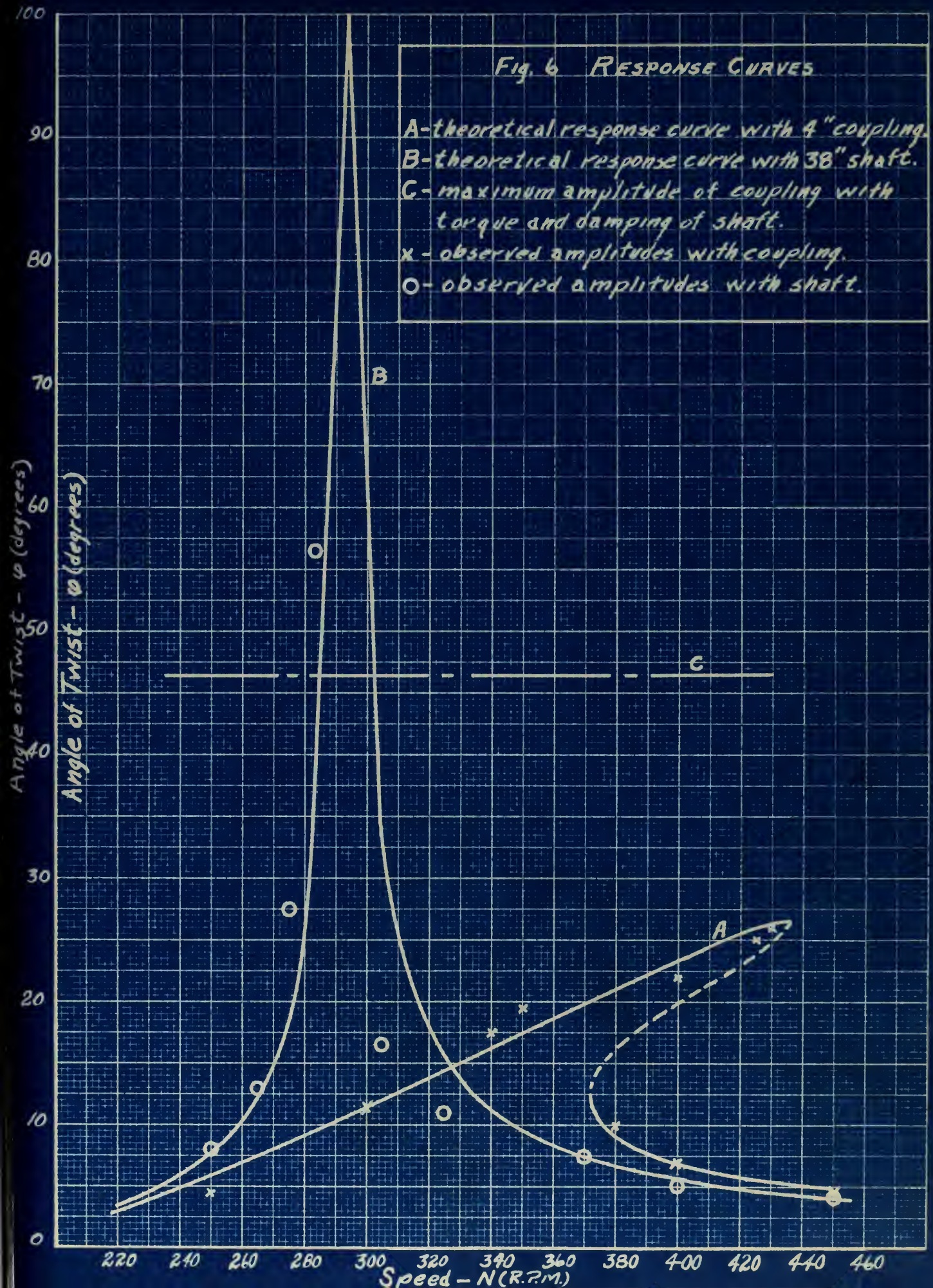
Fig. 6 Response Curves
A-theoretical response curve with 4" coupling.
B-theoretical response curve with 38" shaft.
C-maximum amplitude of coupling with torque and damping of shaft.
x-observed amplitudes with coupling.
O-observed amplitudes with shaft.
Angle of Twist - φ (degrees)
Angle of Twist - ω (degrees)
Speed - N (R.P.M.)
A
B
C
0
10
20
30
40
50
60
70
80
90
100
220
240
260
280
300
320
340
360
380
400
420
440
460

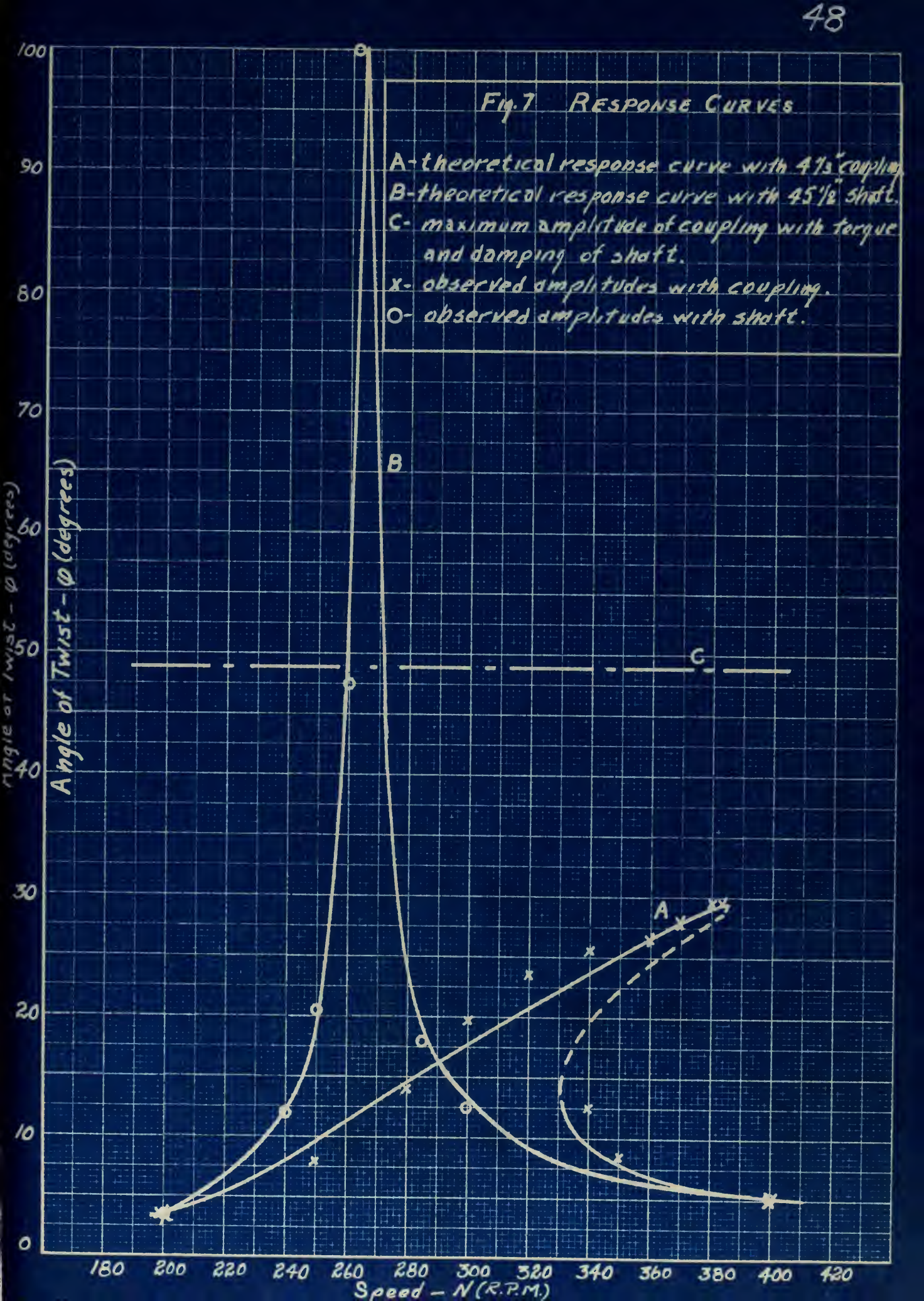
Fig. 7 Response Curves
A- theoretical response curve with 4 7/8" coupling.
B- theoretical response curve with 45/8" shaft.
C- maximum amplitude of coupling with torque and damping of shaft.
x- observed amplitudes with coupling.
O- observed amplitudes with shaft.
Angle of Twist - Ø (degrees)
Speed - N (R.P.M.)
A
B
C
0
10
20
30
40
50
60
70
80
90
100
180
200
220
240
260
280
300
320
340
360
380
400
420

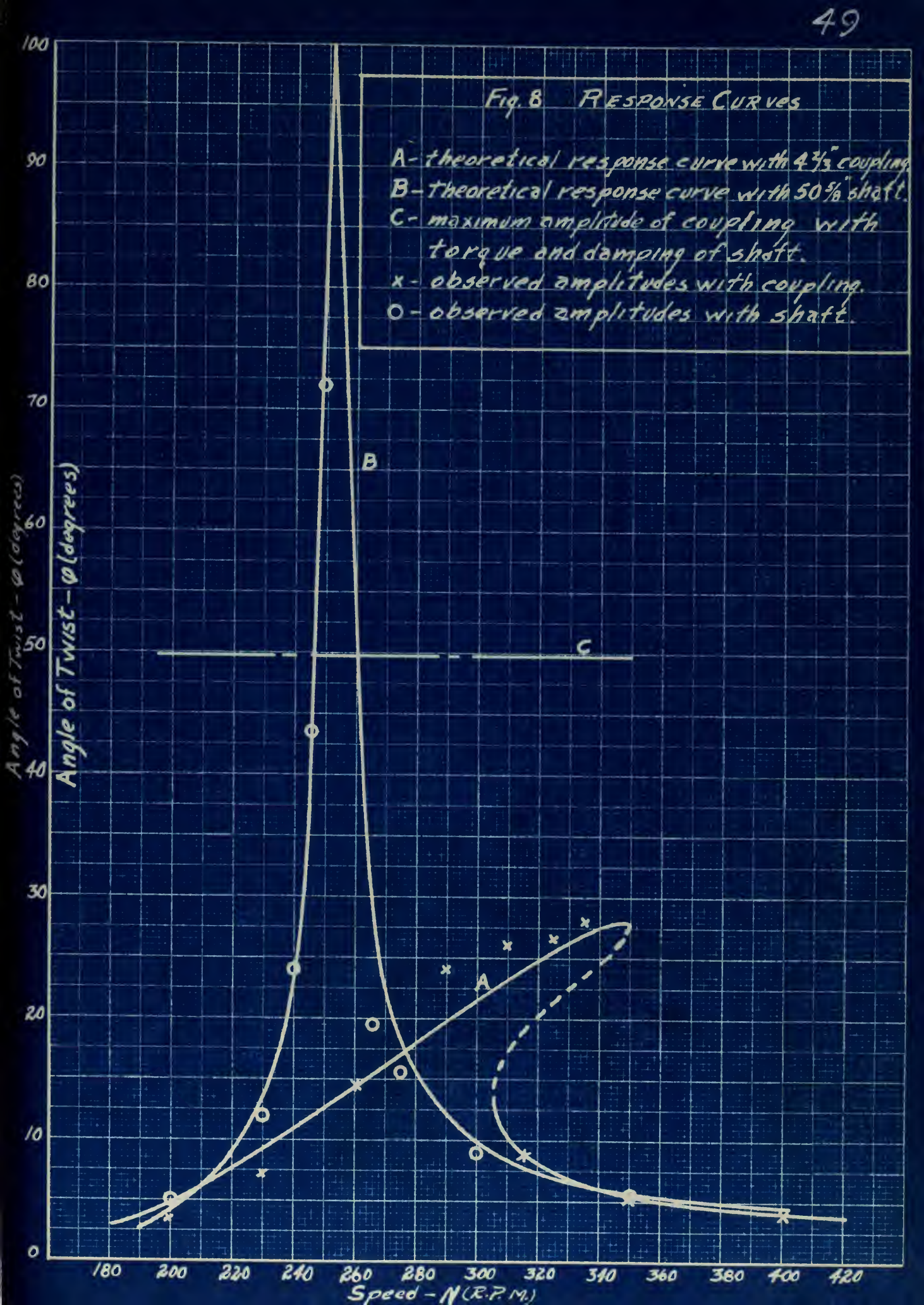
Fig. 8 Response Curves
A - theoretical response curve with 4 3/3" coupling
B - Theoretical response curve with 50 5/8" shaft.
C - maximum amplitude of coupling with torque and damping of shaft.
x - observed amplitudes with coupling.
O - observed amplitudes with shaft.
Angle of Twist - φ (degrees)
Angle of Twist - φ (degrees)
100
90
80
70
60
50
40
30
20
10
0
A
B
C
180
200
220
240
260
280
300
320
340
360
380
400
420
Speed - N (R.P.M.)

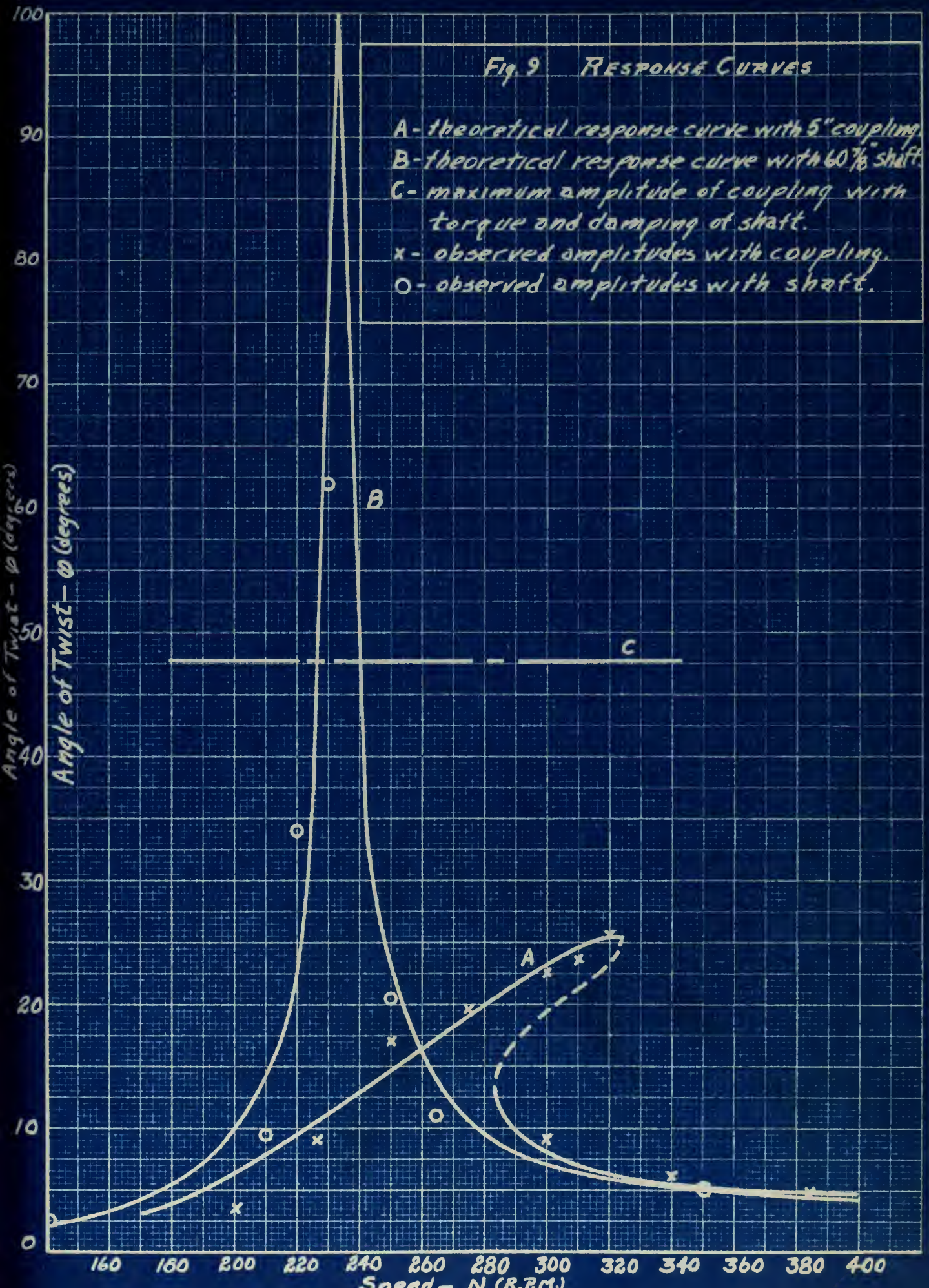
Fig. 9 Response Curves
A - theoretical response curve with 5" coupling
B - theoretical response curve with 60% shaft
C - maximum amplitude of coupling with torque and damping of shaft.
x - observed amplitudes with coupling.
O - observed amplitudes with shaft.
Angle of Twist - Φ (degrees)
Angle of Twist - Φ (degrees)
100
90
80
70
60
50
40
30
20
10
0
A
B
C
160
180
200
220
240
260
280
300
320
340
360
380
400
Speed - N (R.P.M.)

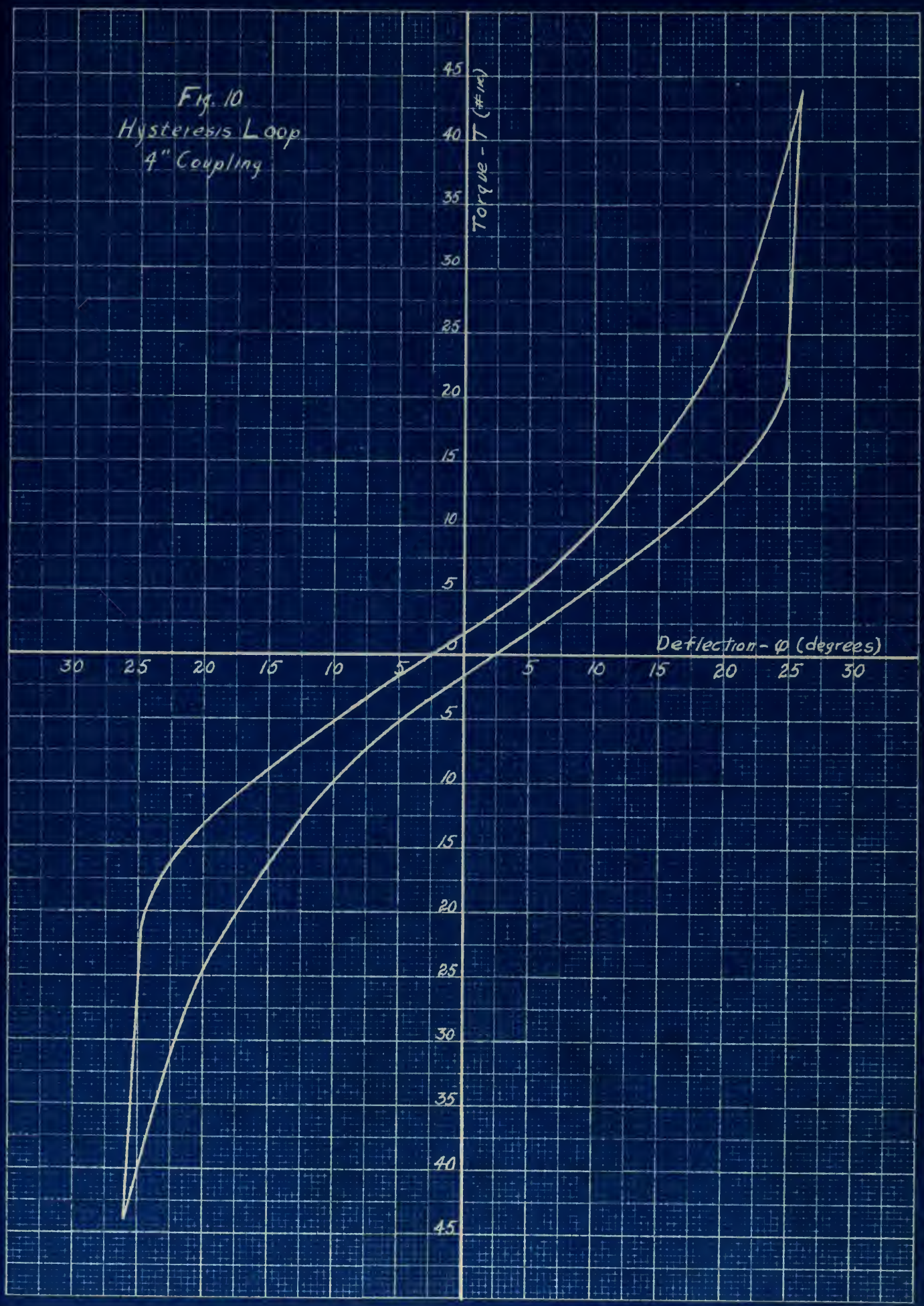
Fig. 10
Hysteresis Loop
4" Coupling
Torque - T (#in)
Deflection - φ (degrees)
45
40
35
30
25
20
15
10
5
0
30
25
20
15
10
5
0
5
10
15
20
25
30
35
40
45

Fig. 11
Hysteresis Loop
4 1/3" Coupling

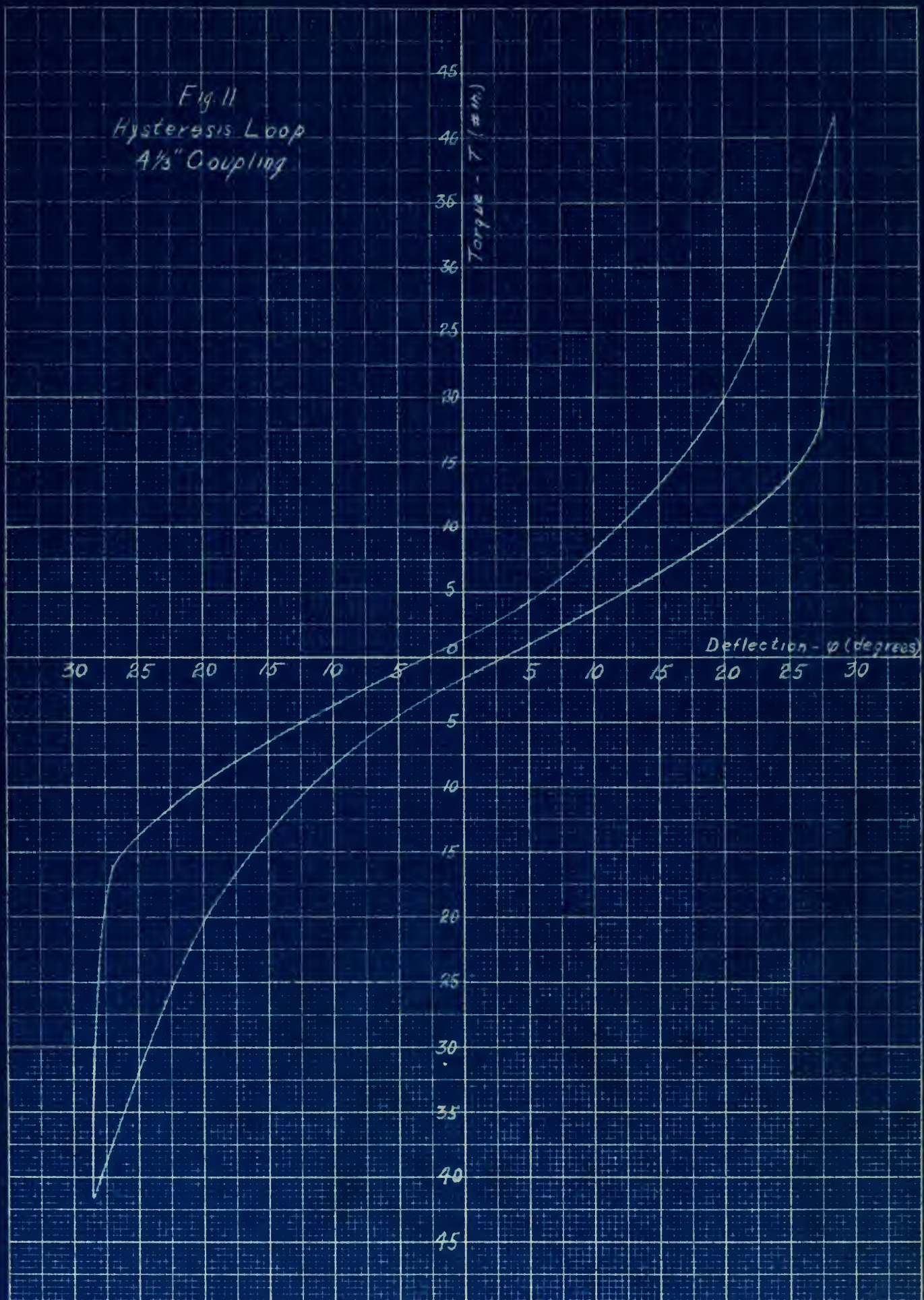

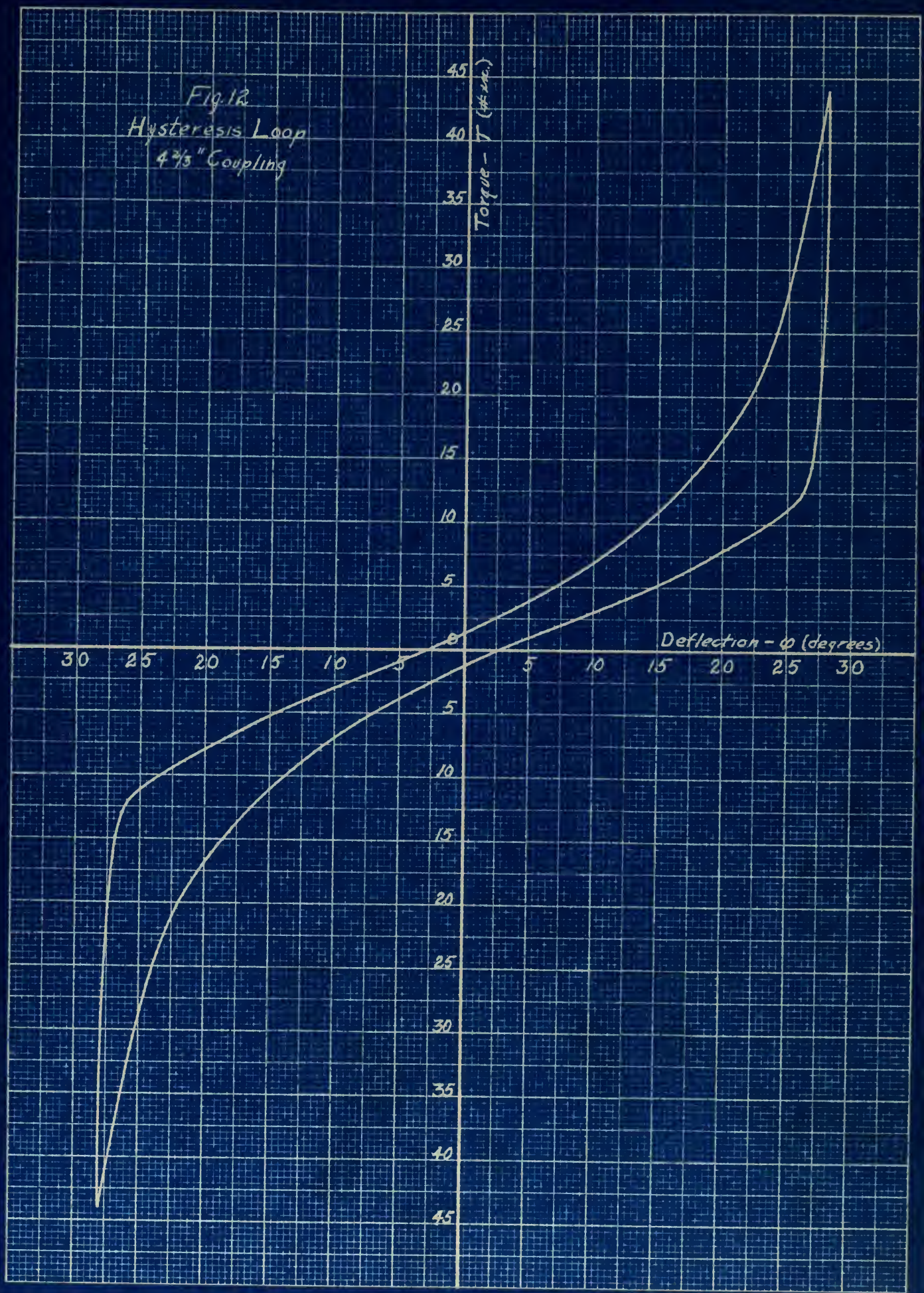
Fig. 12
Hysteresis Loop
4 2/3" Coupling
Torque - T (ft-lbs.)
Deflection - φ (degrees)
45
40
35
30
25
20
15
10
5
0
30
25
20
15
10
5
5
10
15
20
25
30

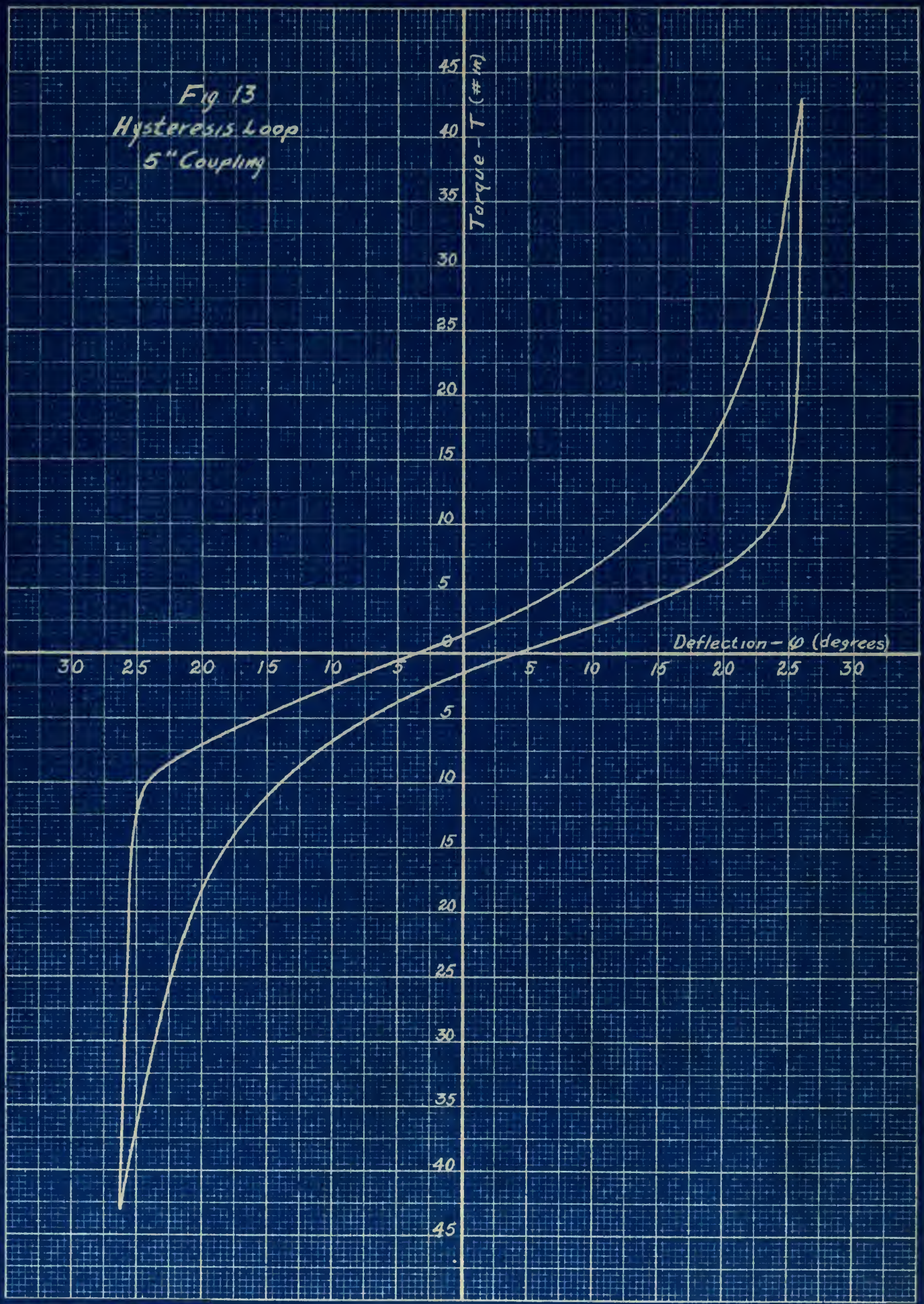
Fig 13
Hysteresis Loop
5" Coupling
Torque - T (#ft)
Deflection - φ (degrees)
45
40
35
30
25
20
15
10
5
0
30
25
20
15
10
5
5
10
15
20
25
30

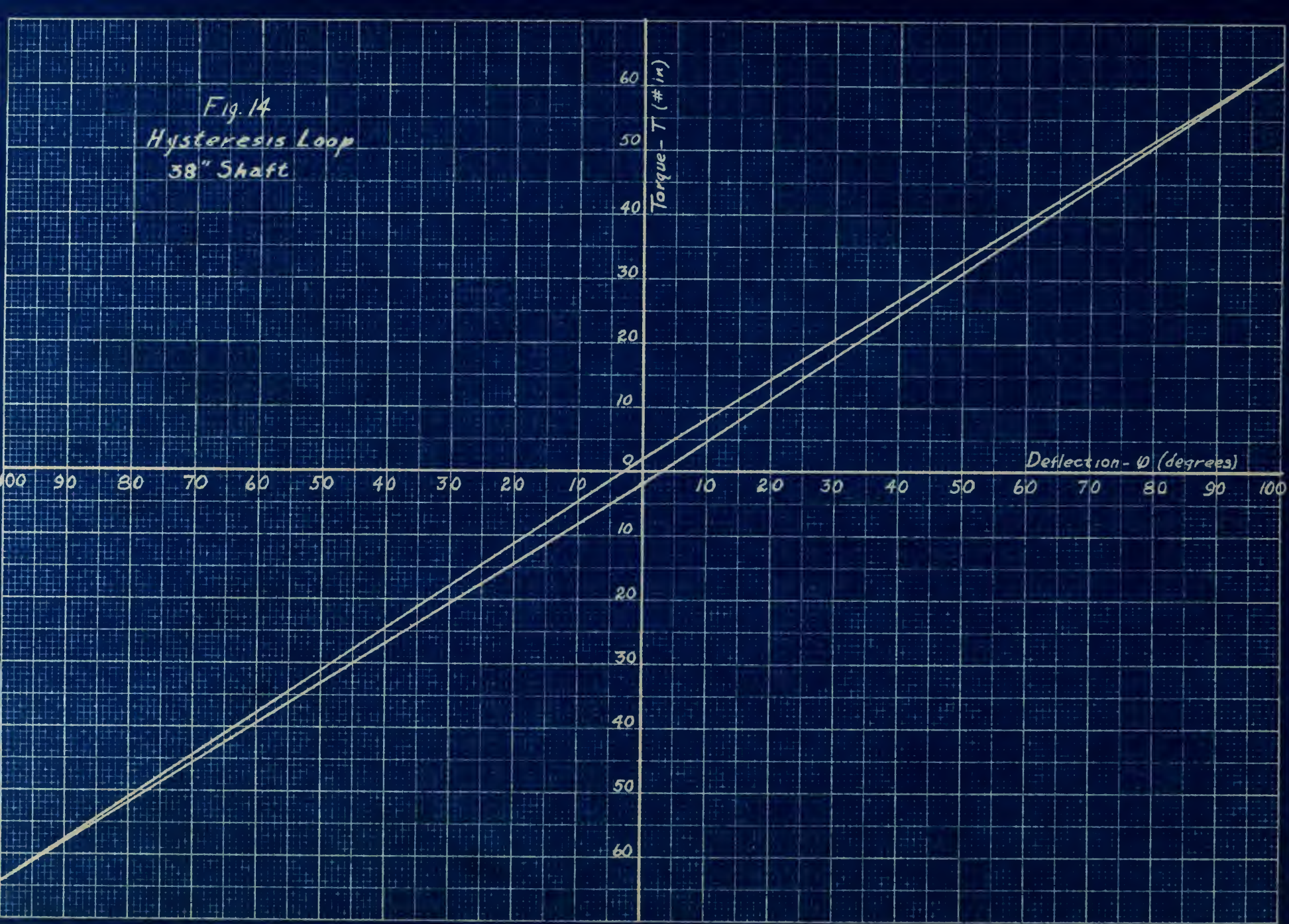
Fig. 14
Hysteresis Loop
38" Shaft
Torque - T (# in)
Deflection - Φ (degrees)
60
50
40
30
20
10
0
10
20
30
40
50
60
70
80
90
100

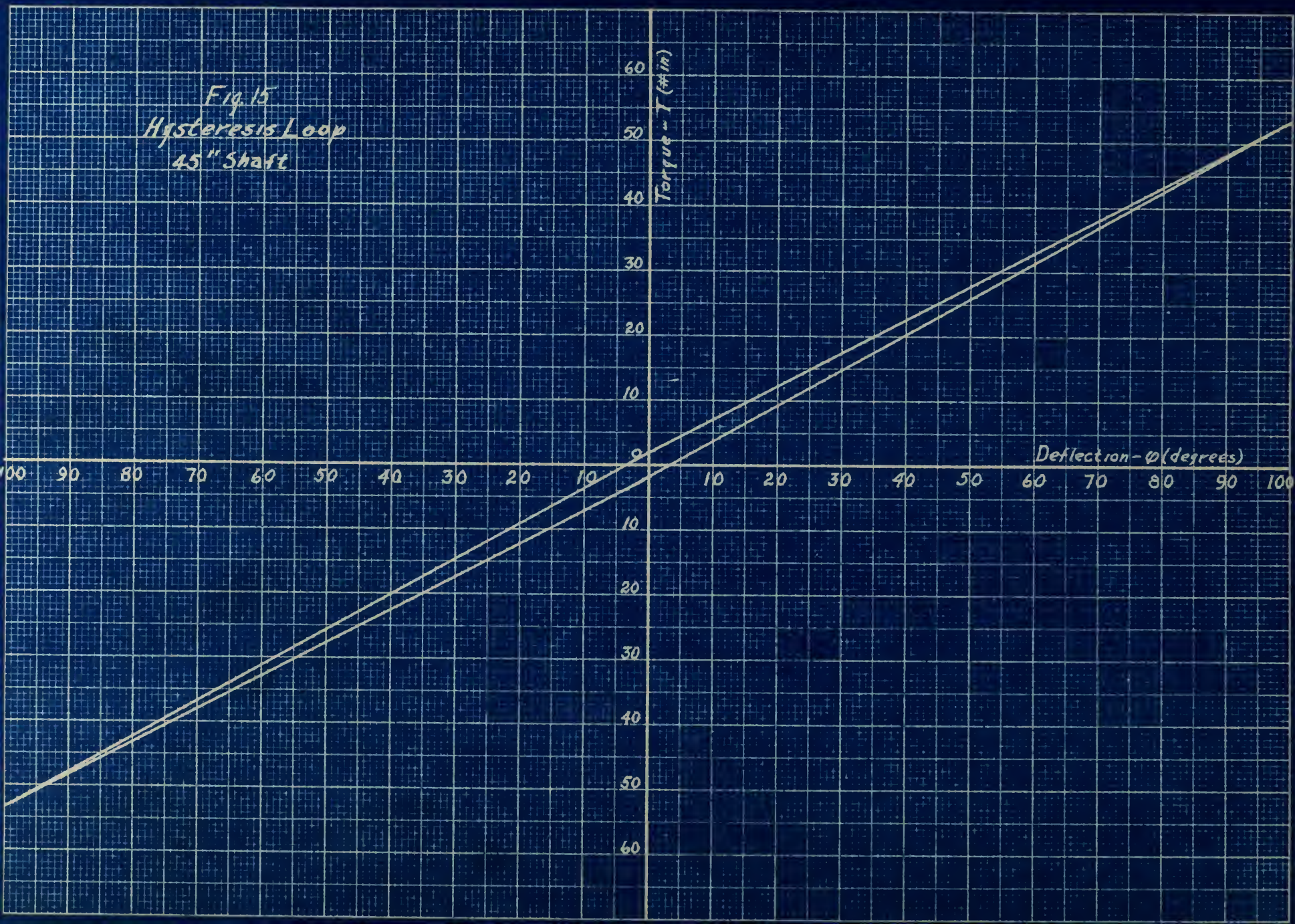
Fig. 15
Hysteresis Loop
45" Shaft
Torque - T (#in)
Deflection - φ (degrees)
60
50
40
30
20
10
0
10
20
30
40
50
60
70
80
90
100

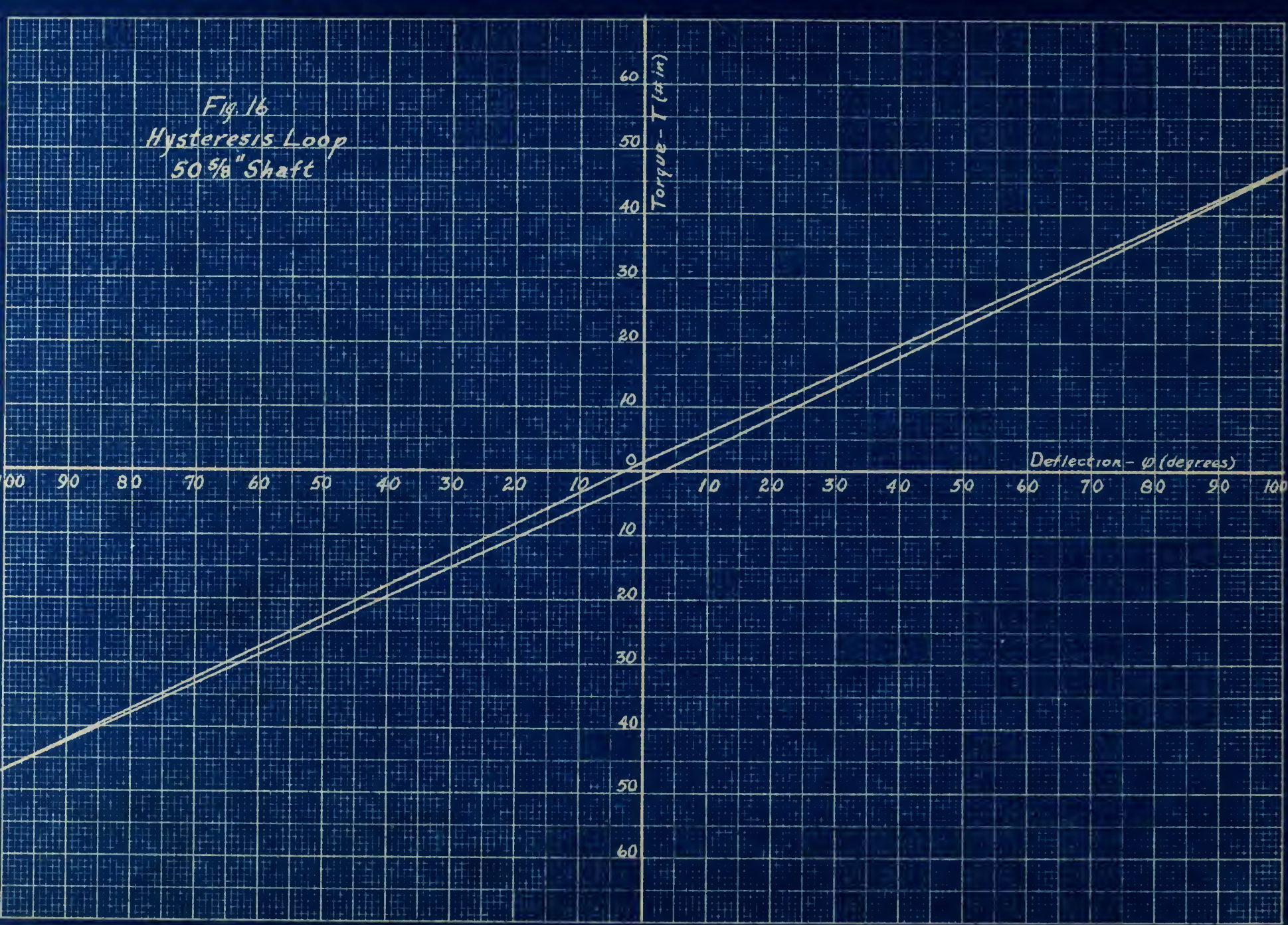
Fig. 16
Hysteresis Loop
50 5/8" Shaft
Torque - T (in)
Deflection - φ (degrees)
60
50
40
30
20
10
0
10
20
30
40
50
60
70
80
90
100

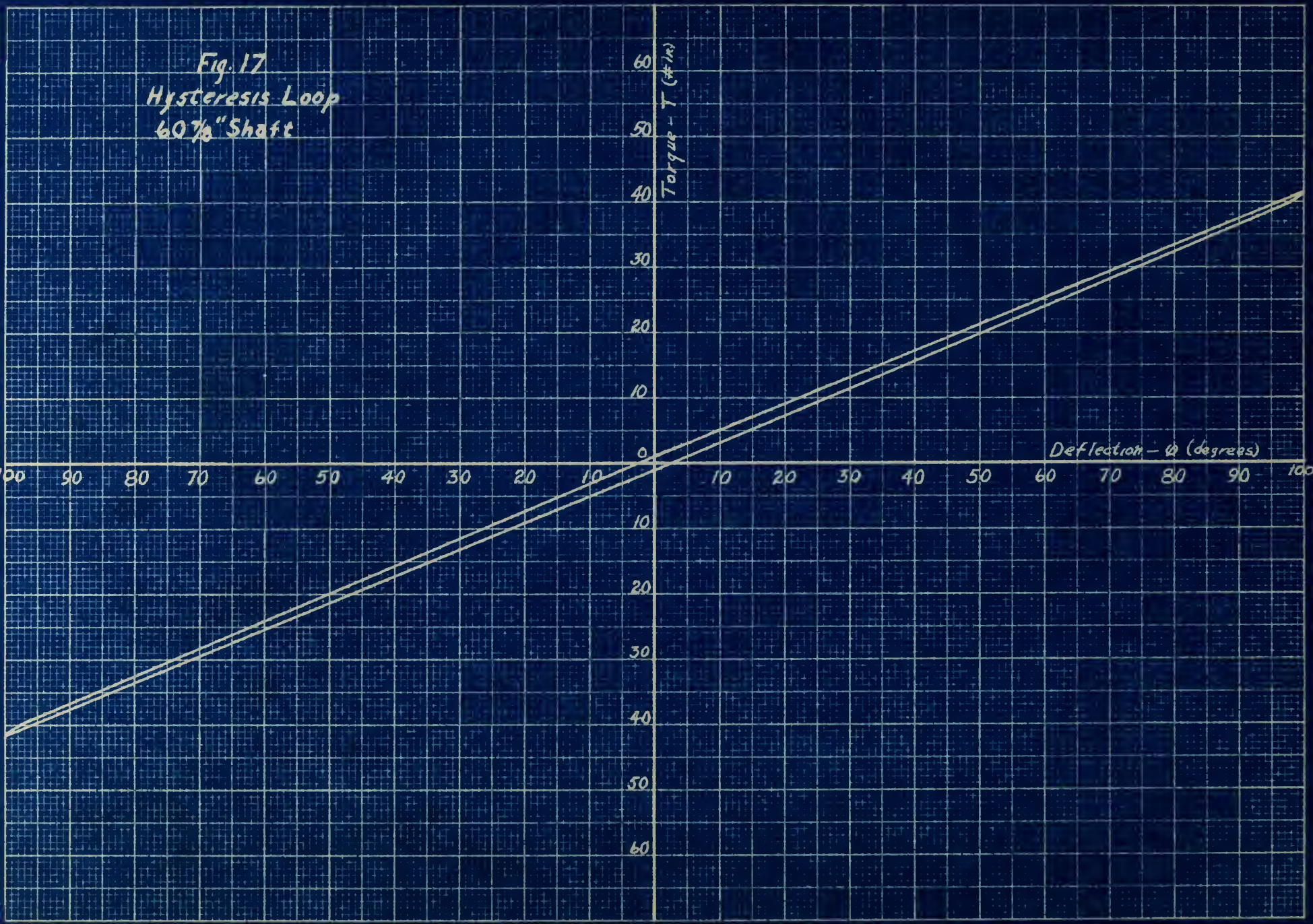
Fig. 17
Hysteresis Loop
60 7/8" Shaft
Torque - T (#in)
Deflection - φ (degrees)
60
50
40
30
20
10
0
10
20
30
40
50
60
90
80
70
60
50
40
30
20
10
10
20
30
40
50
60
70
80
90
100

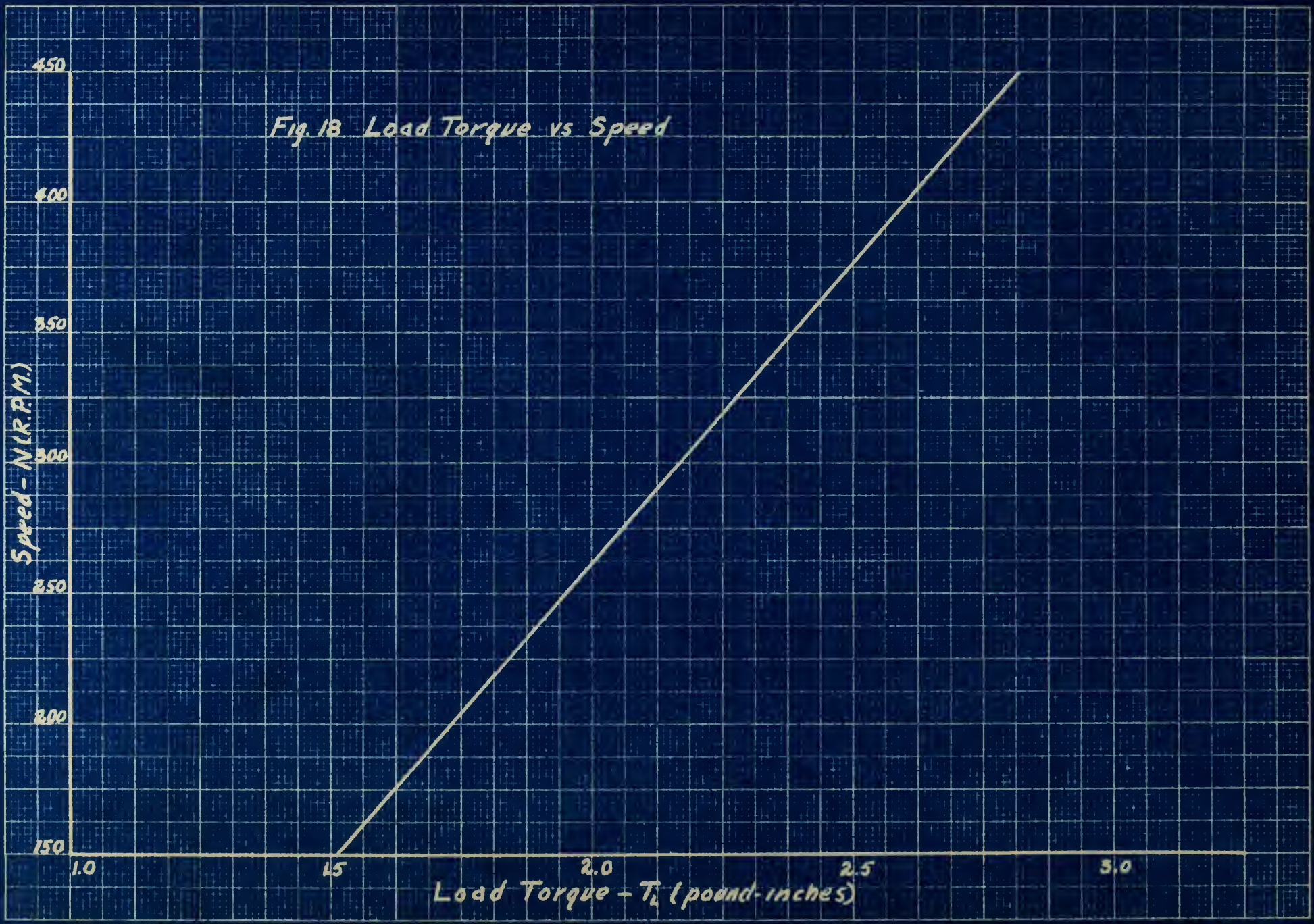
Fig. 18 Load Torque vs Speed
450
400
350
300
250
200
150
Speed - N (R.P.M.)
1.0
1.5
2.0
2.5
3.0
Load Torque - T_L (pound-inches)

Thesis 6310
P4 Peterson
An investigation of vibration phenomena in torsional systems having non-linear spring characteristics.